[21] V. T. Franques and V. K. Jain, "Enhanced wavelet-based zerotree coding of images," in *Proc. of 1996 Data Compression Conference*, 1996, p. 436.

[22] C. S. Barreto and G. V. Mendonca, "Enhanced zerotree wavelet transform image coding exploiting similarities inside subbands," in *Proc. of International Conference on Image Processing*, 1996, vol. 2, pp. 549–551.

[23] X. Wu and J.-H. Chen, "Context modeling and entropy coding of wavelet coefficients for image compression," in *Proc. of 1997 International Conference on Acoustics, Speech, and Signal Processing*, 1997, pp. 3097–3100.

[24] T. Cover and J. Thomas, *Elements of Information Theory*, Wiley, New York, 1991.

[25] J. Rissanen, "Universal coding, information, prediction, and estimation," *IEEE Trans. on Information Theory*, vol. 30, pp. 629–636, July 1984.

[26] *ftp://carlos.wustl.edu*.

[27] A. Said and W. A. Pearlman, "A new fast and efficient image codec based on set partitioning in hierarchical trees," *IEEE Transactions on Circuits and Systems for Video Tech.*, vol. 6, pp. 243–250, June 1996.

[28] Y. Chen and W. A. Pearlman, "Three-dimensional subband coding of video using the zerotree method," in *Visual Communications and Image Processing '96, Proc. of SPIE 2727*, Mar. 1996, pp. 1302–1309.

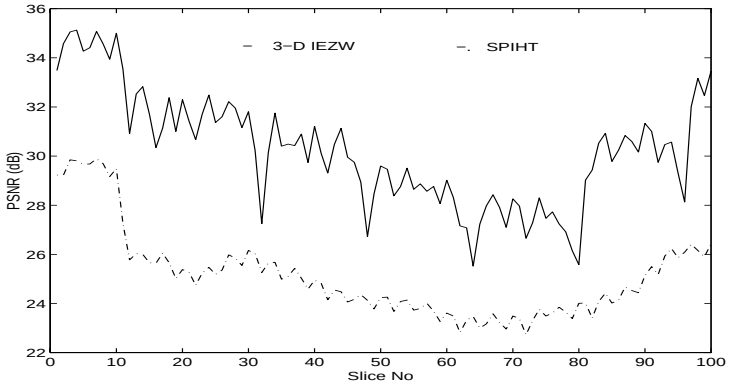

Figure 4: Progressive performance of 3-D IEZW at an average rate of 0.1 bits/pixel.

Figure 5: Left to right: Original slice no. 79 of CT_skull image volume, Slices reconstructed at 0.1 bits/pixel using 2-D SPIHT and 3-D IEZW, respectively.

[2] M. J. Weinberger, G. Seroussi, and G. Sapiro, "LOCO-I: A low complexity, context-based lossless image compression algorithm," in *Proc. of 1996 Data Compression Conference*, 1996, pp. 140–149.

[3] X. Wu and N. Menon, "CALIC-A context based adaptive lossless image codec," in *Proc. of 1996 International Conference on Acoustics, Speech, and Signal Processing*, 1996, pp. 1890–1893.

[4] J. Wang and H. K. Huang, "Medical image compression by using three-dimensional wavelet transformation," *IEEE Transactions on Medical Imaging*, vol. 15, pp. 547–554, Aug. 1996.

[5] J. Luo, X. Wang, C. W. Chen, and K. J. Parker, "Volumetric medical image compression with three-dimensional wavelet transform and octave zerotree coding," in *Proc. of SPIE, Visual Communications and Image Processing '96*, 1996, vol. 2727, pp. 579–590.

[6] B. Aiazzi, P. S. Alba, S. Baronti, and L. Alparone, "Three-dimensional lossless compression based on a separable generalized recursive interpolation," in *Proc. of International Conference on Image Processing*, 1996, vol. 1, pp. 85–88.

[7] M. A. Pratt, C. H. Chu, and S. Wong, "Volume compression of MRI data using zerotrees of wavelet coefficients," in *Proc. of SPIE, Wavelet Applications in Signal and Image Processing IV*, 1996, vol. 2825, pp. 752–763.

[8] A. Baskurt, H. Benoit-Cattin, and C. Odet, "On a 3-D medical image coding method using a separable 3-D wavelet transform," in *Proc. of SPIE, Medical Imaging 95*, 1995, vol. 2431, pp. 184–194.

[9] K. L. Lau, W. K. Vong, and W. Y. Ng, "Lossles compression of 3-D images by variable predictive coding," in *Proc. of 2nd Singapore International Conference on Image Processing*, 1992, pp. 161–165.

[10] A. Zandi, J. D. Allen, E. L. Schwartz, and M. Boliek, "CREW: Compression with reversible embedded wavelets," in *Proc. of Data Compression Conference*, Mar. 1995, pp. 212–221.

[11] A. Said and W.A. Pearlman, "An image multiresolution representation for lossless and lossy compression," *IEEE Transactions on Image Processing*, vol. 5, pp. 1303–1310, Sept. 1996.

[12] S. Dewitte and J. Cornelis, "Lossless integer wavelet transform," *IEEE Signal Processing Letters*, vol. 4, pp. 158–160, June 1997.

[13] R. Calderbank, I. Daubechies, W. Sweldens, and B.-L. Yeo, "Wavelet transforms that map integers to integers," *submitted to Journal of Applied and Computational Harmonics Analysis*.

[14] J. Shapiro, "Embedded image coding using zerotrees of wavelet coefficients," *IEEE Transactions on Signal Processing*, vol. 41, pp. 3445–3462, Dec. 1993.

[15] M. Vetterli and J. Kovacevic, *Wavelets and Subband Coding*, Prentice-Hall, Englewood Cliffs, NJ, 1995.

[16] G. Strang and T. Nguyen, *Wavelets and Filter Banks*, Wellesley-Cambridge Press, Wellesley, MA, 1996.

[17] I. Daubechies and W. Sweldens, "Factoring wavelet and subband transforms into lifting steps," *submitted to Journal of Fourier Analysis and Applications*.

[18] W. Sweldens, "The lifting scheme: A custom-design construction of biorthogonal wavelets," *Journal of Applied and Computational Harmonic Analysis*, vol. 3(2), pp. 186–200, 1996.

[19] J. W. Woods and T. Naveen, "A filter based bit allocation scheme for subband compression of HDTV," *IEEE Trans. on Image Processing*, vol. 1, pp. 436–440, July 1992.

[20] J. Li, P.-Y. Cheng, and C.-C. J. Kuo, "On the improvements of embedded zerotree wavelet (EZW) coding," in *Proc. SPIE, Visual Communications and Image Processing '95*, 1995, vol. 2501, pp. 1490–1501.

2-level dyadic decompositions. Of the transforms considered in this work, all but the (2,2) and S transforms performed similarly. The (2,2) and S transforms are low order transforms and were not able to decorrelate the images as effectively as other higher order transforms. There was no single transform that performed best over the entire data set. This is consistent with the 2-D results obtained in [13].

Table 1: Comparison of different methods on CT and MR data (in bits/pixel averaged over the entire image volume).

FileName	Volume Size	UNIX Compress	LOCO-I [2]	CALIC [3]	3-D EZW	3-D CB-EZW
CT_skull	256 x 256 x 192	4.1357	2.8460	2.7250	2.3571	**2.2005**
CT_wrist	256 x 256 x 176	2.7204	1.6531	1.6912	1.3947	**1.2723**
CT_carotid	256 x 256 x 64	2.7822	1.7388	1.6547	1.6017	**1.5279**
CT_Aperts	256 x 256 x 96	1.7399	1.0637	1.0470	1.0600	**0.9879**
MR_liver_t1	256 x 256 x 48	5.304	3.1582	3.0474	2.5451	**2.3983**
MR_liver_t2e1	256 x 256 x 48	3.9384	2.3692	2.2432	1.9446	**1.8220**
MR_sag_head	256 x 256 x 16	3.5957	2.5567	2.5851	2.3224	**2.2279**
MR_ped_chest	256 x 256 x 64	4.3338	2.9282	2.8102	2.1764	**2.0225**

Table 2: Comparison of different integer wavelet transforms on CT data (in bits/pixel averaged over the entire image volume).

FileName	(2,2)	(4,2)	(2,4)	(6,2)	(2+2,2)	S	S+P
CT_skull	2.9519	2.2210	**2.2005**	2.2773	2.2942	2.7976	2.2046
CT_wrist	1.8236	1.3057	**1.2723**	1.3391	1.3448	1.6756	1.3274
CT_carotid	2.1408	1.5136	1.5279	1.5491	1.5289	1.8524	**1.4553**
CT_Aperts	1.4263	1.0416	0.9879	1.0776	**0.9717**	1.1826	1.0139
MR_liver_t1	3.2270	2.4262	**2.3983**	2.4687	2.4707	3.1384	2.4156
MR_liver_t2e1	2.5771	1.7607	1.8220	1.7704	1.8810	2.3701	**1.7530**
MR_sag_head	2.8631	2.4254	2.2279	2.4547	**2.1955**	2.7353	2.3569
MR_ped_chest	2.4954	2.1489	**2.0225**	2.1960	2.0586	2.4927	2.1174

5.2. Progressive Performance

As discussed earlier, the proposed algorithm produces an embedded bitstream, enabling progressive decoding. In this section, we present the progressive performance of our algorithm. No attempt has been made to optimize the technique for progressive transmission. This is a topic for future research.

Figure 4 shows the progressive performance of the 3-D CB-EZW algorithm at an average rate of 0.1 bits/pixel. For reference, the results using the 2-D Set Partitioning in Hierarchial Trees (SPIHT) algorithm [27] are included. As before, this application of SPIHT does not exploit the dependencies in the third dimension.

These results show that the proposed algorithm offers excellent lossy performance, even at low bit rates. The average PSNR for the 3-D CB-EZW is roughly 5 dB and 4 dB better than that of 2-D SPIHT at 0.1 and 0.5 bits/pixel, respectively. It should also be noted that the progressive performance of the 3-D CB-EZW declines sharply at the boundaries of the 16 slice coding unit. Similar observations were also made in [28]. Improving the progressive performance at these coding unit edges remains a topic of future research.

Figure 5 shows slice number 79 of the CT_skull data set, together with reconstructed images at 0.1 bits/pixel using 2-D SPIHT and 3-D CB-EZW, respectively.

6. REFERENCES

[1] S. Wong, L. Zaremba, D. Gooden, and H. K. Huang, "Radiologic image compression - A review," *Proc. of the IEEE*, vol. 83, pp. 194–219, Feb. 1995.

$P(x|C)$, which has to be estimated on the fly through past observations. A better estimate of $P(x|C)$ yields a better coding performance. Since the amount of data necessary to reliably estimate $P(x|C)$ increases with increasing model order, higher-order modeling contexts can result in many symbols being coded using inaccurate probability estimates. This problem is known as context dilution [25]. Context dilution is especially important in cases where the source is not stationary. Here, rapid adaptation of the modeling context histograms is essential. Furthermore, the memory requirements to store this model at both the encoder and the decoder grow exponentially with respect to the order. Computational requirements also increase with increasing model order, since higher order models require more computations to compute the index to the probability table corresponding to the current context.

For context-based adaptive arithmetic coding of EZW symbols, the context models can be designed to take advantage of the spatial and hierarchical dependencies, as well as dependencies across subbands at the same level of the transform. The wavelet coefficients around the current coefficient can be used to exploit the spatial dependencies, and the parent coefficient can be used to exploit the hierarchial dependencies. Similarly, the dependencies across subbands at the same level can be exploited using the coefficients at the same spatial location in the image. Any combination of these coefficients can be used to create the current context. However, it is important to preserve causality in context models, since the decoder needs to be able to reproduce the context at every symbol to decode.

5. RESULTS

We have performed coding experiments on several 8-bit CT and MR image volumes obtained from Mallinckrodt Institute of Radiology Image Processing Laboratory [26]. Table 5.1 illustrates the lossless performance of the algorithm presented here together with two other algorithms found in the literature. Both LOCO-I [2] and CALIC [3] are state-of-the-art 2-D lossless compression algorithms and are included in the table for reference. The results for these algorithms were obtained by encoding every slice independently and averaging the bit rate over the entire image volume. This is not an entirely fair comparison as LOCO-I and CALIC make no attempt to exploit dependencies in the third dimension.

The EZW and context-based EZW (CB-EZW) are the 3-D techniques presented in this paper. The 3-D EZW algorithm does not have context modeling, and the adaptive arithmetic coder is reset at every subband. The 3-D CB-EZW algorithm uses context modeling as described in the previous section. We use the three causal 4-connected symbols around the symbol to be encoded, as well as the parent symbol. For the purpose of forming the context, the 4-connected symbols are allowed to be one of POS, NEG, IZ, or ZTR, where as the parent is identified only as significant, or insignificant. This scheme results in $2 \times 4^3 = 128$ contexts.

The results in Table 5.1 were obtained using a 2-level dyadic implementation of the (2,4) integer wavelet transform on consecutive volumes of 16 slices. The same transform was used in all three directions. The bitrate is averaged over the entire image volume. It should also be noted that all of the results given in this paper are computed from actual file sizes, not entropies. The results show that the exploitation of dependencies in the third dimension significantly improves performance. The compressed files for 3-D CB-EZW are on average 14% and 20% smaller for the CT and MR data sets, respectively, compared to the smallest file from the two 2-D techniques. It can also be seen that the utilization of contexts provides additional gain in coding performance. The files for 3-D CB-EZW are on average 7% and 6% smaller than the files for 3-D EZW for CT and MR data sets, respectively.

5.1. Performance Using Different Integer Wavelet Transformations

In this section, we present the performance of our algorithm using different integer wavelet transforms. The results presented in Table 5.1 were obtained using the 3-D CB-EZW algorithm, and use

In a dyadic wavelet transform, every coefficient is related to a set of coefficients at the next finer level that correspond to the same spatial location in the image. A coefficient at a coarse level is called a *parent*, while its spatially related coefficients at the next finer level are referred to as its *children*. This dependency can be represented using a tree structure. Notice that for 2-D data coefficients in the lowpass band at the coarsest scale have only three children, where all the other coefficients, except for the coefficients at the finest scale, have four. The coefficients at the finest scale are childless. All the coefficients at finer levels that descend from a coefficient at a coarse level are called its *descendants*.

Embedded Coding of Zerotrees of Wavelet Coefficients (EZW), which was introduced by Shapiro in [14], is based on the observation that if a coefficient is small in magnitude with respect to a threshold, then all of its descendants are likely to be small as well. EZW suggests an efficient way of ordering the bits of the wavelet coefficients for transmission. The reader is referred to [14] for a detailed explanation and a simple example of the EZW algorithm.

The extension of the method of [14] to a three-dimensional wavelet transform is straight forward. The parent-children relations are considered in three dimensions, instead of two. Figure 3 illustrates such a tree structure. Note that the root node of the tree has only seven children, while all other nodes, except the leaves, have eight. In other words, except for the root node, and the leaves, a coefficient at (x, y, z) has the coefficients at

$$\begin{aligned}(2x, 2y, 2z), (2x+1, 2y, 2z), (2x, 2y+1, 2z), (2x, 2y, 2z+1), (2x+1, 2y+1, 2z),\\ (2x+1, 2y, 2z+1), (2x, 2y+1, 2z+1), (2x+1, 2y+1, 2z+1)\end{aligned} \tag{30}$$

as its children. To define the parent-children relationship for a coefficient at the root node, let L_x, L_y, L_z be the dimensions of the root subband. Then, a coefficient of the root subband at (x, y, z) has the coefficients at

$$\begin{aligned}(x+L_x, y, z), (x, y+L_y, z), (x, y, z+L_z), (x+L_x, y+L_y, z),\\ (x+L_x, y, z+L_z), (x, y+L_y, z+L_z), (x+L_x, y+L_y, z+L_z)\end{aligned} \tag{31}$$

as its children. Clearly, the leaf nodes do not have any children.

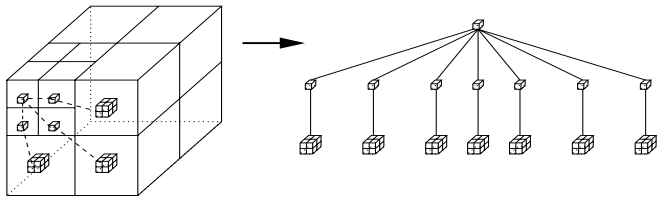

Figure 3: Three-dimensional tree structure.

4.1. Context-Based Three-Dimensional Zerotree Coding

Several improvements to two-dimensional EZW have been suggested recently [20, 21, 22, 23]. In this work, we improve the performance of three-dimensional EZW by using context-based adaptive arithmetic coding, which exploits dependencies between symbols.

The fundamental problem in context-based adaptive arithmetic coder design is to select good modeling contexts. Let x be the symbol we want to encode. A simple memoryless model is not usually efficient, and would require $-\log_2(P(x))$ bits to encode this symbol. A better choice is to use a high-order model. We create a modeling context, $C = \{x_1, x_2, \cdots, x_K\}$, where x_i are symbols for other coefficients that depend on the current symbol. Then, $-\log_2(P(x|C))$ bits are needed to encode x. Note that if each x_i has B bits of resolution, then there are 2^{BK} different contexts.

In theory, the higher the order of the modeling context, the lower the conditional entropy [24]. However in practice, increasing the order of the modeling context does not always improve the coding performance. The arithmetic coder requires an estimate of the statistical model of the source,

We also consider two other integer wavelet transforms in the literature:

• The S transform, (1,1):

$$d[n] = x[2n+1] - x[2n] \tag{22}$$

$$s[n] = x[2n] + \lfloor \frac{1}{2} d[n] \rfloor. \tag{23}$$

• An S+P transform [11], (4,2):

$$d^{(1)}[n] = x[2n+1] - x[2n] \tag{24}$$

$$s[n] = x[2n] + \lfloor \frac{d^{(1)}[n]}{2} \rfloor \tag{25}$$

$$d[n] = d^{(1)}[n] + \lfloor \frac{2}{8}(s[n-1] - s[n]) + \frac{3}{8}(s[n] - s[n+1]) + \frac{2}{8} d^{(1)}[n+1] + \frac{1}{2} \rfloor. \tag{26}$$

4. ZEROTREE CODING

Progressive transmission is a highly desirable feature for many image compression applications. For progressive transmission, the information in the bitstream is arranged in order of importance. More important information appears at the beginning of the bitstream, while less important information appears towards the end. A coarse version of the image can therefore be recovered by decoding the initial portion of the bitstream, and the image can be refined by continuing the decoding process, until perfect reconstruction is achieved.

If mean-squared error (MSE) is selected as the distortion measure, information that provides greater decrease in MSE is considered more important. Let $\mathbf{I}$ be the original image, and $\mathbf{T}$, an orthonormal transform. Then the transform coefficients $\mathbf{C}$ are given by

$$\mathbf{C} = \mathbf{T}\mathbf{I}. \tag{27}$$

Let $\hat{\mathbf{C}}$ denote the approximation of $\mathbf{C}$ produced at the decoder. Then, the reconstructed image $\hat{\mathbf{I}}$ is given by

$$\hat{\mathbf{I}} = \mathbf{T}^{-1}\hat{\mathbf{C}}. \tag{28}$$

The MSE between the original and reconstructed images is given by

$$MSE = \frac{1}{N}\|\mathbf{I} - \hat{\mathbf{I}}\|^2 = \frac{1}{N}\|\mathbf{C} - \hat{\mathbf{C}}\|^2 = \frac{1}{N}\sum_m \sum_n |C(m,n) - \hat{C}(m,n)|^2 \tag{29}$$

where N is the number of pixels in the image, and $C(m,n)$ denotes the transform coefficient at wavelet coordinate (m,n). Equation (29) follows from the fact that orthonormal transforms preserve the L_2 norm.

If the decoder initially sets all of the coefficients to zero and updates them progressively, it follows from Equation (29) that the coefficient with the largest magnitude needs to be transmitted first, since it would provide the largest reduction in MSE. This approach could be further improved by the following observation: If the coefficients are represented in binary notation, the bits that are '1's at higher bit planes provide greater reduction in MSE than the '1' bits at lower bit planes, when transmitted. This observation suggests that we should transmit the '1' bits at the highest bit plane first, rather than transmitting all the bits of the coefficient with the largest magnitude. It should also be noted that when the decoder receives these bits, it should be able to locate the coefficients that each bit belongs to. Thus some additional information needs to be transmitted to denote the order in which these bits were transmitted.

For non-orthonormal transforms, the MSE in $\hat{\mathbf{I}}$ can often be computed as a *weighted* MSE in $\hat{\mathbf{C}}$ [19], i.e., by weighting each term of the sum in (29). Although the transforms used in this work are non-orthonormal, this weighting is not used here. This is a topic of on-going research.

and

$$s^{(i)}[n] = s^{(i-1)}[n] - \lfloor (\sum_k u^{(i)}[k] d^{(i)}[n-k]) + \frac{1}{2} \rfloor \tag{8}$$

respectively. The inverse is obtained by reversing the lifting, and the dual lifting steps, and flipping signs,

$$s^{(i-1)}[n] = s^{(i)}[n] + \lfloor (\sum_k u^{(i)}[k] d^{(i)}[n-k]) + \frac{1}{2} \rfloor \tag{9}$$

and

$$d^{(i-1)}[n] = d^{(i)}[n] + \lfloor (\sum_k p^{(i)}[k] s^{(i-1)}[n-k]) + \frac{1}{2} \rfloor . \tag{10}$$

It should be noted that although integers are transformed to integers, the coefficients $p^{(i)}[k]$ and $u^{(i)}[k]$ are not necessarily integers. Thus, computing the integer transform coefficients requires floating point operations.

In this work we use the following integer wavelet transforms of [13] with the notation $(N, \tilde{N})$, where N and $\tilde{N}$ represent the number of vanishing moments of the analysis and synthesis high pass filters, respectively:

- A (2,2) transform:

$$d[n] = x[2n+1] - \lfloor \frac{1}{2}(x[2n] + x[2n+2]) + \frac{1}{2} \rfloor \tag{11}$$

$$s[n] = x[2n] + \lfloor \frac{1}{4}(d[n-1] + d[n]) + \frac{1}{2} \rfloor . \tag{12}$$

- A (4,2) transform:

$$d[n] = x[2n+1] - \lfloor \frac{9}{16}(x[2n] + x[2n+2]) - \frac{1}{16}(x[2n-2] + x[2n+4]) + \frac{1}{2} \rfloor \tag{13}$$

$$s[n] = x[2n] + \lfloor \frac{1}{4}(d[n-1] + d[n]) + \frac{1}{2} \rfloor . \tag{14}$$

- A (2,4) transform:

$$d[n] = x[2n+1] - \lfloor \frac{1}{2}(x[2n] + x[2n+2]) + \frac{1}{2} \rfloor \tag{15}$$

$$s[n] = x[2n] + \lfloor \frac{19}{64}(d[n-1] + d[n]) - \frac{3}{64}(d[n-2] + d[n+1]) + \frac{1}{2} \rfloor . \tag{16}$$

- A (6,2) transform:

$$d[n] = x[2n+1] - \lfloor \frac{75}{128}(x[2n] + x[2n+2]) - \frac{25}{256}(x[2n-2] + x[2n+4]) \tag{17}$$

$$+ \frac{3}{256}(x[2n-4] + x[2n+6]) + \frac{1}{2} \rfloor$$

$$s[n] = x[2n] + \lfloor \frac{1}{4}(d[n-1] + d[n]) - \frac{1}{2} \rfloor . \tag{18}$$

- A (2+2,2) transform:

$$d^{(1)}[n] = x[2n+1] - \lfloor \frac{1}{2}(x[2n] + x[2n+2]) + \frac{1}{2} \rfloor \tag{19}$$

$$s[n] = x[2n] + \lfloor \frac{1}{4}(d^{(1)}[n-1] + d^{(1)}[n]) + \frac{1}{2} \rfloor \tag{20}$$

$$d[n] = d^{(1)}[n] - \lfloor \frac{1}{16}(-s[n-1] + s[n] - s[n+1] - s[n+2]) + \frac{1}{2} \rfloor . \tag{21}$$

wavelet transform. They showed that any discrete wavelet transform can be computed using this scheme and almost all these transforms have reduced computational complexity compared to the standard filtering algorithm. In this scheme, a trivial wavelet transform, called the lazy transform, is computed first. This transform simply splits the input into two by gathering the even and odd indexed samples in separate arrays. Let $x[n]$ be the input signal. Then the lazy wavelet transform is given by

$$s^{(0)}[n] = x[2n] \tag{1}$$

and

$$d^{(0)}[n] = x[2n+1]. \tag{2}$$

Next, alternating "dual lifting" and 'lifting" steps are applied to obtain

$$d^{(i)}[n] = d^{(i-1)}[n] - \sum_k p^{(i)}[k] s^{(i-1)}[n-k] \tag{3}$$

and

$$s^{(i)}[n] = s^{(i-1)}[n] - \sum_k u^{(i)}[k] d^{(i)}[n-k]. \tag{4}$$

where the coefficients $p^{(i)}[k]$ and $u^{(i)}[k]$ are computed using a lifting factorization of the polyphase matrix. The reader is referred to [17] for details. Figure 2 illustrates this process using M pairs of dual lifting and lifting steps.

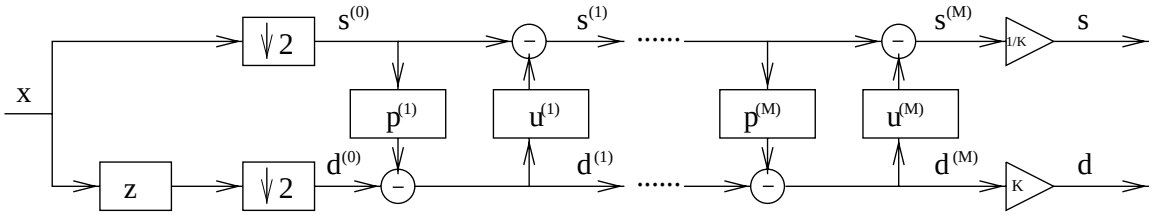

Figure 2: The forward wavelet transform using lifting.

Finally, the samples $s^{(M)}[n]$ become the low pass coefficients $s[n]$, while the samples $d^{(M)}[n]$ become the high pass coefficients $d[n]$ when scaled with a factor K,

$$s[n] = \frac{s^{(M)}[n]}{K} \tag{5}$$

and

$$d[n] = K d^{(M)}[n]. \tag{6}$$

For the transforms considered in this work, $K = 1$.

For the inverse transform, the operations of the forward transform are reversed.

3. INTEGER WAVELET TRANSFORMS

In most cases, the wavelet transform produces floating point coefficients, and although this allows perfect reconstruction of the original image in theory, the use of finite-precision arithmetic, together with quantization, results in a lossy scheme.

Recently, new wavelets that transform integers to integers have been introduced [10, 11, 12, 13]. In [13], it was shown that an integer version of every wavelet transform with finite filters can be obtained using the lifting scheme of [18].

Integer wavelet transforms, i.e., wavelet transforms that transform integers to integers, can be developed using the lifting scheme by rounding off the result of each dual lifting and lifting step before adding or subtracting. In particular, the dual lifting and lifting steps are replaced by

$$d^{(i)}[n] = d^{(i-1)}[n] - \lfloor (\sum_k p^{(i)}[k] s^{(i-1)}[n-k]) + \frac{1}{2} \rfloor \tag{7}$$

anatomically. A better approach is to consider the whole set of slices as a three-dimensional volume. In the literature, several methods that utilize dependencies in all three dimensions have been proposed [4, 5, 6, 7, 8, 9]. Some of these methods [4, 5, 7, 8] use three-dimensional discrete wavelet transforms in lossy schemes, while others [6, 9] use predictive coding to achieve lossless compression.

In this work, we introduce a lossless three-dimensional wavelet compression algorithm that exploits the dependencies in all three dimensions of volumetric medical images. We decompose the image data into subbands using a three-dimensional integer wavelet transform [10, 11, 12, 13]. We then use a generalization of the the zerotree coding scheme of [14] together with context-based adaptive arithmetic coding to encode the subband coefficients. The algorithm produces an embedded bitstream, and thus allows progressive reconstruction of images. In other words, it is possible to reconstruct a lossy version of the image volume, by decoding the initial portion of the bitstream. The quality of the image volume can be improved by further decoding of the bitstream, until the images are perfectly reconstructed.

Results for a set of CT and MR images are presented using different wavelet transforms. We also investigate the lossless performance of the algorithm as well as its progressive performance and compare with other compression techniques.

2. WAVELET TRANSFORMS

The wavelet transform is a valuable tool for multiresolution analysis and has been widely used in image compression applications [15, 16]. In transform coding of images, the image is projected onto a set of basis functions and the resulting transform coefficients are encoded. Efficient coding requires that the transform compact the energy in a small number of coefficients and have good localization in both the space and spatial-frequency domains.

The wavelet transform can be implemented using perfect reconstruction FIR filter banks and extended to multi-dimensions using seperable filters [15, 16]. Each dimension is filtered and downsampled separately. Figure 1 illustrates the implementation of two levels of a three-dimensional dyadic decomposition.

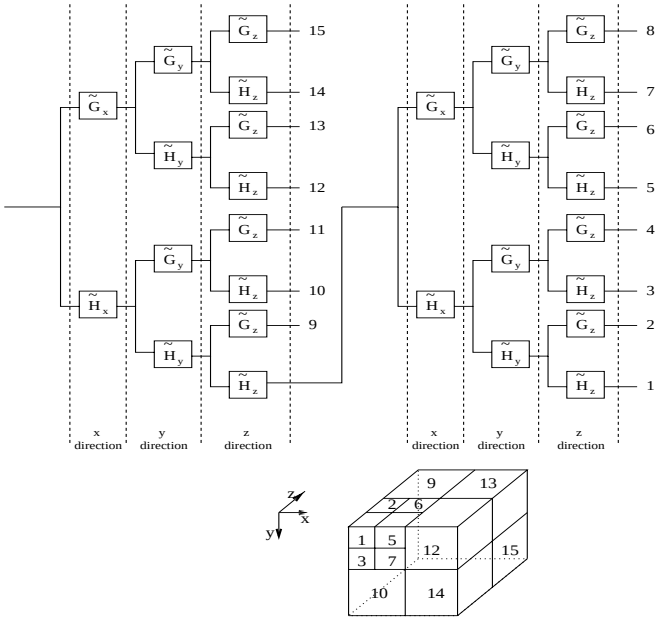

Figure 1: Three-dimensional Wavelet Analysis.

In [17], Daubechies and Sweldens present a scheme, called *lifting*, for computing the discrete

EFFICIENT LOSSLESS CODING OF MEDICAL IMAGE VOLUMES USING REVERSIBLE INTEGER WAVELET TRANSFORMS

Ali Bilgin, George Zweig[†]*, Michael W. Marcellin*

Dept. of Electrical and Computer Engineering, University of Arizona, Tucson, AZ 85721.
[†] Los Alamos National Laboratory, Los Alamos, NM 87545
and Signition, Inc., 901 18^{th} St., Los Alamos, NM 87544.

ABSTRACT

A novel lossless medical image compression algorithm based on three-dimensional integer wavelet transforms and zerotree coding is presented. The EZW algorithm is extended to three dimensions and context-based adaptive arithmetic coding is used to improve its performance. The algorithm (3-D CB-EZW) efficiently encodes image volumes by exploiting the dependencies in all three dimensions, while enabling lossy and lossless compression from the same bitstream. Results on lossless compression of CT and MR images are presented, and compared to other lossless compression algorithms. The progressive performance of the 3-D CB-EZW algorithm is also compared to other lossy progressive coding algorithms. For representative images, the 3-D CB-EZW algorithm produced an average of 14% and 20% decrease in compressed file sizes for CT and MR images, respectively, compared to the best available 2-D lossless compression techniques.

1. INTRODUCTION

An increasing number of medical radiology images are created directly in digital form. Clinical picture archiving and communication systems (PACS), and telemedicine networks require the storage and transmission of a large amount of medical image data, and efficient compression of these data are crucial. Several techniques for their compression have been proposed [1]. These can be classified into lossless and lossy techniques. Lossless techniques allow exact reconstruction of the original image, while the lossy techniques aim to achieve high compression ratios by allowing some acceptable degradation in the image.

Although lossy compression is gaining acceptance, lossless compression has been widely preferred by medical professionals for several reasons [1]. Since lossless compression does not degrade the image, it facilitates accurate diagnosis. Many physicians fear that lossy compression techniques might lead to errors in diagnosis, since in some cases they can introduce unknown artifacts, although in most cases they achieve excellent visual quality. Furthermore, there exists several legal and regulatory issues that favor lossless compression.

Several of today's diagnostic imaging techniques, such as computed tomography (CT), magnetic resonance (MR), positron emission tomography (PET), and single photon emission computed tomography (SPECT), produce a three-dimensional volume of the object being imaged, represented as multiple two-dimensional slices. These images can be coded independently on a slice by slice basis. There exist several 2-D lossless compression algorithms, such as the LOw COmplexity LOssless COmpression of Images (LOCO-I) algorithm [2] and the Context-based, Adaptive, Lossless Image Codec (CALIC) algorithm [3], that produce excellent results. However, such two-dimensional methods do not benefit from exploiting the dependencies that exist among all three dimensions. Since the image slices are cross sections that are parallel and adjacent to one another, they are correlated

Part of this work was performed while the first author was at Los Alamos National Laboratory. This work was supported in part by the Department of Energy Applied Mathematics Program, the Naval Research Laboratory, — Stennis Space Center, and the National Science Foundation under Grant No. NCR-9258374. E-mail: {bilgin,mwm}@ece.arizona.edu, zweig@busco.lanl.gov. URL: http://www-spacl.ece.arizona.edu.